International Journal of GEOMATE, June 2019, Vol.16, Issue 58, pp.62 - 68
Geotec., Const. Mat. & Env., DOI: https://doi.org/10.21660/2019.58.8152
ISSN: 2186-2982 (Print), 2186-2990 (Online), Japan

EFFECTS OF THRUST PROTECTING METHOD FOR BURIED PIPE USING GEOGRID GABION OF DIFFERENT SIZES

*Hiroyuki Araki[1] and Daiki Hirakawa[1]

[1]Department of Civil and Environmental Engineering, Chuo University, Japan

*Corresponding Author, Received: 22 June 2018, Revised: 13 July 2018, Accepted: 20 Dec. 2018

ABSTRACT: On the bend of a buried water supply pipeline, the thrust force is applied to the ground. A concrete block is typically installed at the bend section of the pipeline as a thrust protection measure. However, a concern exists that the stability of the concrete block might not be maintained when the ground around the concrete block liquefies during an earthquake. In this study, thrust protection using a gabion composed of a geogrid basket and gravel as a pressure-receiving structure to protect against thrust force is proposed. Further, the effects of this method are evaluated by conducting model experiments. In the model experiments, a constant load simulated thrust force was applied laterally to a buried pipe model in the model ground where the internal effective stress was decreased by increasing hydraulic gradient stepwise. Gabion models of several widths were placed on the ground in the direction of the thrust force. Results revealed that the gabion stabilizes the pipe even when the effective pressure of the surrounding ground decreases significantly and that the behavior of gabions in the ground is affected by their width. Moreover, the requirements for a gabion to improve a pipe's stability will be discussed herein, based on the results of several test cases.

Keywords: Buried pipe, Thrust force, Gabion, Liquefaction

1. INTRODUCTION

At the bend of buried pipes in which pressurized water flows, the thrust force caused by the centrifugal force due to the water flow or the imbalance of the water pressure is applied to the ground outside the bend. In design, the stability of the bend is typically judged by considering the passive earth pressure of the ground and the frictional force between the pipe and the ground as the resistance force against the thrust force. If the thrust force exceeds the resistance force, a thrust-protecting method is applied.

A concrete block is typically used as the thrust-protecting method and is installed at the bend, as shown in Fig. 1a. The concrete block expands the pressure-receiving area of the passive earth pressure and increases the frictional resistance force at the bottom by its weight. However, this protecting method has several problems. The resistance force decreases markedly in the liquefied ground because the frictional force and passive earth pressure are lost. Further, the high inertial force is generated at the bend where the weight is increased by the concrete block. The high inertial force promotes the deformation of the buried pipe. A pipeline damaged in this manner by the inertial force was reported in a past earthquake [1].

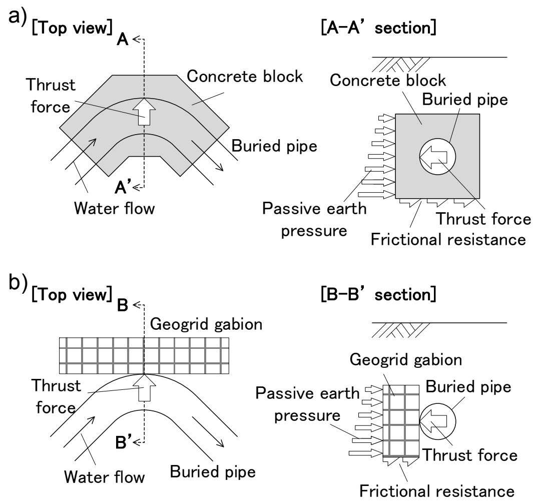

Fig. 1 Schematics of a) a concrete block and b) the proposed method using gabion.

A new thrust-protecting method, other than a concrete block, is therefore required to attain the following performances goals: exerting sufficient resistance force against the thrust under normal conditions, retaining the resistance force to prevent significant deformation during an earthquake, and obtaining the resistance force without increasing the weight of the pipe to not grow the inertial force acting on the buried pipe. Kawabata et al. [2]

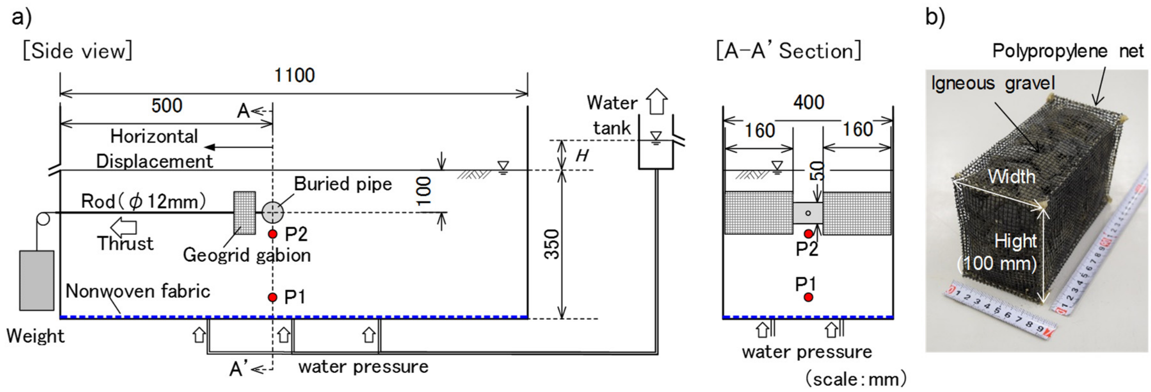

Fig. 2 a) Schematics of the lateral load test and b) photograph of geogrid gabion model (1.5D width).

proposed a new thrust-protecting method using a geogrid, in which the geogrid is connected to the pipe on the inside of the bend to act as a lateral anchor. They also observed the behavior of a pipe protected by the geogrid in the liquefied ground by conducting shaking table tests [3]. It was revealed that the lateral displacement of a pipe protected with the geogrid decreased, compared to that of a pipe protected with a concrete block.

In this study, another type of thrust-protection method is proposed. A geogrid gabion consisting of gravel and a basket constructed from geogrid is installed at the passive area of the buried pipe to receive the thrust force as shown in Fig. 1b. In a previous study [4], it was clarified that the displacement of a pipe was decreased by applying a gabion. In this study, the effects of the gabion size on the thrust protection are clarified by conducting model experiments.

2. THE PROPOSED THRUST PROTECTING METHOD

If the passive earth pressure is not sufficient to overcome the thrust force from a buried pipe, the ground in the passive area of the buried pipe deforms. Audibert et al. [5] reported that the deformation region was developed from the lateral face of the buried pipe toward the ground surface in the passive area. In the proposed method, the geogrid gabions are installed in the passive area, as shown in Fig. 1b.

The gabion is a basket filled with igneous gravel. The basket is constructed of a polymer geogrid to obtain long-term stability against environmental changes. The gabion is not deformed largely by the thrust force because the gravel material is confined by the geogrid basket. The passive earth pressure indirectly acting on the buried pipe is expected to be increased by a gabion height that is larger than the pipe diameter. Using gravel material of high permeability as the filling material, the excess pore water pressure around the buried pipe is expected to be dispersed to retain effective stress during an earthquake. These mechanisms might ensure resistance to the thrust force without increasing the weight of the bend.

By conducting the model experiments, it was confirmed that the lateral displacement of a pipe with a gabion decreased compared to that of a pipe without a gabion in the ground where the effective stress decreased [4]. It was concluded that the effects of installing a gabion were due to the increase in the passive earth pressure and the suppression of the local shear deformation of the ground near the buried pipe. However, the effects of the gabion width were not clarified.

3. OUTLINE OF LATERAL LOAD TEST

3.1 Test Conditions

Although the dynamic interaction between a structure and the ground is typically investigated by shaking table tests, the results obtained by such tests are the behaviors in a complicated boundary field where the force acting on the buried pipe changes sequentially. The buried pipe might be affected by not only the thrust force but also the inertial force, which varies hourly.

Herein, the effects of the gabion size on the thrust protection are evaluated by lateral load tests, with reference to Itani et al. [6]. The lateral load tests were conducted in a testing box as shown in Fig. 2a. The pipe model was loaded laterally inside the ground model where the effective stress is controlled by excess pore water pressure.

The ground model was of sandy soil (soil particle density, $\rho_s = 2.680$ g/cm^3) with particle size distribution as shown in Fig. 3. The maximum dry density and the optimum water content of the sandy soil were 1.616 g/cm^3 and 17.2%, respectively. The ground model was created by wet tamping using sandy soil with a water content of 17%. The dry density of the ground model was 1.374 g/cm^3.

In the lateral load test, the three-dimensional interaction between the bend and the ground was simplified to the plane strain problem. Hence, the shape of the pipe model was set as a straight cylindrical shape of 50 mm in diameter and having a length of 390 mm. The pipe model was of solid aluminum to prevent its deformation by loading. The pipe model was subjected to a simulated thrust force laterally-applied via a stainless-steel rod. The simulated thrust force was set as 125 N based on the result of the pre-test in which the pipe model moved significantly.

The gabion model was of igneous gravel (ρ_s = 2.795 g/cm^3) and polypropylene net as shown in Fig. 2b. The particle size distribution of the gravel is shown in Fig. 3. The dry density of the gabion was set as approximately 1.39 g/cm^3. The gabions were installed on the front side of thrust force such that the center of gravity position was at the same height as that of the pipe model. Although the gabions should be installed close to the pipe when in actual use, the gabion model was placed with lateral distance to the pipe set as approximately 15 mm to ensure good compaction around the pipe in these tests. In addition, the gabion model was divided into two in the horizontal direction to avoid contacting the loading rod (Fig. 2a).

To prevent the migration of soil into the gabions, a non-woven fabric was laid on only their upper surface. The non-woven fabric was not installed on the side and bottom sections so as to simplify the boundary condition between the gabion and soil in the model test. The ground surface settlement due to the soil migration was not observed in the all-model test in this paper.

3.2 Test Cases and Procedure

Four test cases were set as given in Table 1. Case N1 is the test without a countermeasure. In cases, A3, B5, and C1, gabions of widths 25 mm, 50 mm, and 75 mm were used, respectively. Using the pipe diameter value of 50 mm, the values of the gabion

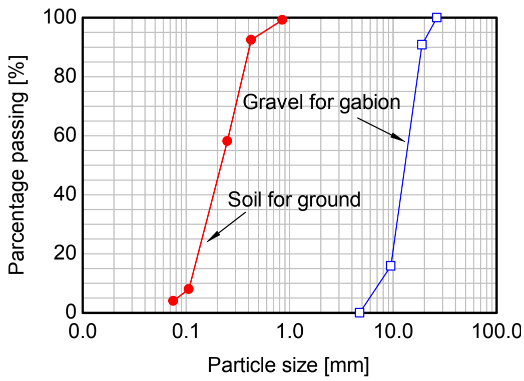

Fig. 3 Particle size distribution of soils used in the model experiments.

Table 1 List of the model experiments.

	Width of gabion	Thrust force [N]	Step No.
Case N1	—	125	1-3
Case A3	0.5D	125	1-7
Case B5	1.0D	125	1-8
Case C1	1.5D	125	1-8

D: a pipe diameter of 50 mm.

Table 2 Test conditions at each step.

Step No.	*H* [mm]	Water condition
1	—	Unsaturated, $w = 17\%$
2	70	Saturated
3	140	Saturated
4	210	Saturated
5	280	Saturated
6	350	Saturated
7	420	Saturated
8	490	Saturated

widths are represented hereafter as 0.5D, 1.0D, and 1.5D respectively. The height of all gabions is 100 mm.

The ground model was saturated with water through the water tank connected to the bottom of the testing box. By increasing the water head difference, defined as H, between the ground surface and the water tank stepwise, as shown in Fig. 2, the excess pore water pressure inside the ground model statically increased; subsequently, the effective stress decreased. The values of H and the water condition at each step are listed in Table 2. The value of H was maintained until the pore water pressure in the ground became stable. After the water pressure stabilized, the pipe model was loaded laterally and the displacement of the model pipe, d_p, was measured. The loading was finished when the value of d_p exceeded 25 mm or when a sand boil occurred in the ground.

The deformation of the ground along with the moving pipe was observed at the side of the testing box. The markers were installed on the side of the testing box and moved following the deformation of the ground. The displacement of the markers was measured by image analysis of the photographs obtained during the loading.

4. TEST RESULTS AND DISCUSSION

4.1 Hydraulic Gradient and Pipe Displacement

The pore water pressure in the model ground was measured by water pressure meters P1 and P2 shown in Fig. 2. Assuming that the distribution of the pore water pressure in the ground is linear with the depth, the hydraulic gradient, i_m was obtained based on the values of excess pore water pressure measured by P1 and P2. Meanwhile, the theoretical value of the critical hydraulic gradient, i_{cr} is expressed by the following equation:

$$i_{cr} = \frac{\rho_s/\rho_w - 1}{1+e} \tag{1}$$

where ρ_s = 2.680 g/cm^3; water density, ρ_w = 1.000 g/cm^3; and the void ratio, e = 0.951 in these test cases. Subsequently, the value of i_{cr} is 0.861. The value of i_m normalized by i_{cr} is equivalent to the ratio of excess pore water pressure to the effective overburden stress in the ground; subsequently, the value of i_m/i_{cr} of 1.0 means that the ground is liquefied.

The relationships between i_m/i_{cr} and H are shown in Fig. 4. The values of i_m/i_{cr} increase linearly as the values of H increase. This indicates that the effective stress in the ground model decrease as the value of H increases. For cases B5 and C1, the values of i_m/i_{cr} were approximately 0.9 at H = 420 mm (step 8), indicating that the ground models were almost liquified.

The relationships between d_p and i_m/i_{cr} are shown in Fig. 5. In all cases, the values of d_p were approximately 4 mm for the unsaturated condition (step 1). The values of d_p hardly increased even when the value of i_m/i_{cr} was 0.0 (step 2). In case N1, however, the pipe moved remarkably at step 3, where the value of i_m/i_{cr} was 0.16. Simultaneously, the values of d_p were approximately 5 mm in cases A3, B5, and C1. In the ground where the value of i_m/i_{cr} was approximately 0.2, the value of the displacements of pipes protected with the gabions having a width of 0.5D to 1.5D were small compared to that without a gabion, and the effect on the displacement resistance of the gabion hardly depended on those widths.

In case A3 using the gabion of 0.5D width, the pipe moved gradually with the increase in i_m/i_{cr} and displaced 23 mm when the value of i_m/i_{cr} was 0.7. Meanwhile, in cases B5 and C1 using the gabion of 1.0D and 1.5D widths, respectively, the values of d_p were approximately 10 mm even when the values of i_m/i_{cr} were approximately 0.9. The effect on the pipe displacement resistance of the gabion of 0.5D width is smaller than that of the 1.0D and 1.5D width gabions.

4.2 Behavior of Gabion in the Ground

To evaluate the behavior in the ground and the gabions, the distributions of the maximum shear

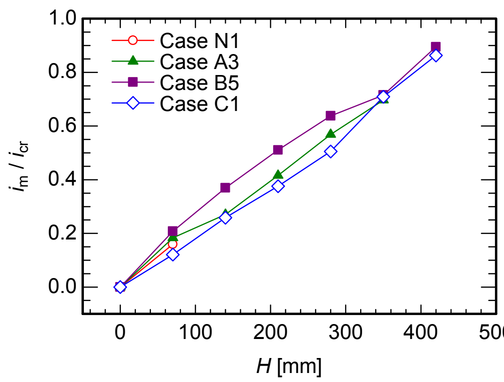

Fig. 4 Relationships between H and i_m/i_{cr}.

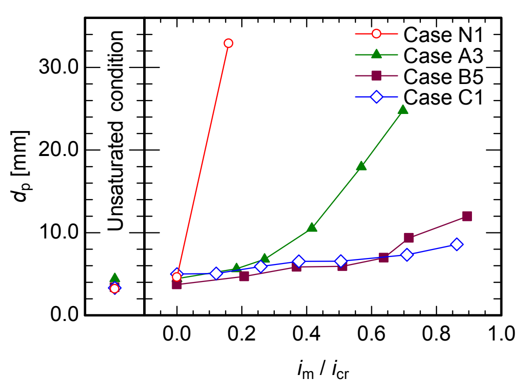

Fig. 5 Relationships between i_m/i_{cr} and d_p.

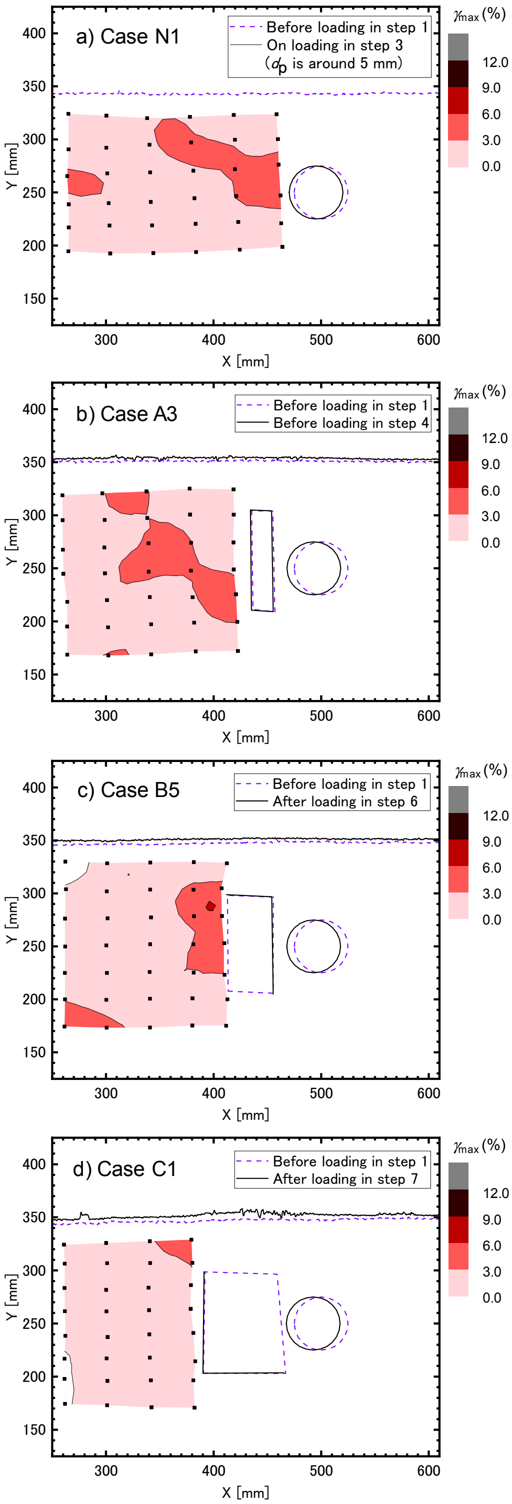

Fig. 6 Distribution of maximum shear strain when d_p is 5 mm to 7 mm.

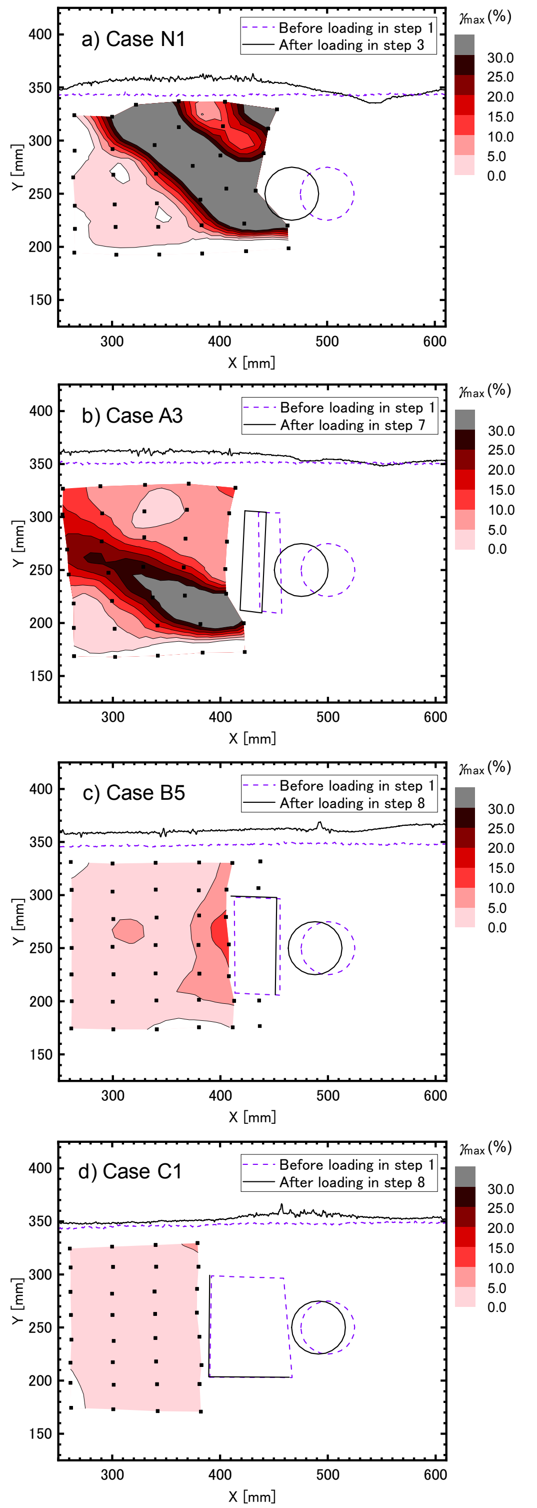

Fig. 7 Distribution of maximum shear strain at the end of each final step

strain, γ_{max} in the ground were calculated based on the displacement of the markers in the model ground. The strain calculation was performed based on each of the four-node rectangular elements using four markers. The distributions of γ_{max} when d_p is 5 mm to 7 mm, and at the end of each final step are shown in Figs. 6 and 7, respectively. The black squares in Figs. 6 and 7 indicate the locations of the markers. The ground surface shapes were also shown in Figs. 6 and 7.

The ground deformation and the behavior of the model pipe without a gabion are shown in Figs. 6a and 7a. The region with a high shear strain was strip-shaped and was distributed from the front of the buried pipe to the ground surface. The ground surface of the upper part of the passive area of the pipe was swollen at the end of step 3 (Fig. 7a).

In case of A3, the shear deformation spread from the bottom of the 0.5D width gabion to the ground surface with the increase in the pipe displacement (Figs. 6b and 7b). The location of the gabion shown in Fig. 7b indicates that the gabion was rotating clockwise. In cases B5 and C1, meanwhile, the gabions with a width of 1.0D and 1.5D, respectively, hardly moved, even at the end of step 8 where the values of i_m/i_{cr} were approximately 0.9 (Figs. 7c, d). The high shear strain region from the bottom of the gabion to the ground surface, such as that shown in Fig. 7b, was also not observed in cases B5 and C1.

The phase of the gabion behavior changed significantly between cases A3 and B5. The difference in the test conditions between cases A3 and B5 was the bottom area of the gabion to which the bottom frictional resistance was applied. The bottom frictional resistance is considered to have influenced the rotational behavior of the gabion. The width might be required to be at least 1.0D to obtain a bottom frictional resistance sufficient to prevent the rotational behavior of the gabion under this experimental condition.

The shear strain was also localized at the side of the 1.0D width gabion in case B5, shown in Figs. 6c and 7c, although the location of the gabion hardly changed compared to that of before loading in step 1. The high shear strain at the side of the gabion suggests the bending deformation of the gabion by the thrust force from the pipe. In case of C1, meanwhile, the shear strain at the side of the gabion was not localized, and remained under 5.0% throughout, even at the end of step 8. The gabion might be required to have a width of 1.5D to prevent the bending deformation by increasing the bending stiffness of the gabion under this experimental condition.

The relationships between i_m/i_{cr} and d_p shown in Fig. 5 were different for cases A3 and B5; subsequently, the pipe displacement was affected strongly by the rotating behavior of the gabion. Moreover, the effect of the bending deformation on the pipe displacement resistance is likely smaller than that of the rotational movement, causing the relationships between i_m/i_{cr} and d_p to be similar to each other in cases B5 and C1. Therefore, it is important to prevent rotation of the gabion to retain the displacement resistant effect in the ground where the effective stress decreases.

5. CONCLUSION

Model experiments were conducted on a new thrust protection method using geogrid gabions to evaluate the effect of the gabion width. The conclusions are summarized as follows:

1) In the ground where the value of i_m/i_{cr} was more than 0.2, the values of the displacements of pipes protected with gabions having a width of 0.5D to 1.5D were small compared to that without a gabion.
2) For the gabion with 0.5D, the pipe displacement increased gradually, and the gabion moved rotationally as the effective stress decreased in the ground.
3) For the gabions with 1.0D and 1.5D widths, the displacements of the pipe were significantly small, and the rotating behavior of the gabion was hardly observed. It is important to prevent the rotating behavior of the gabion to retain the displacement resistant effect.
4) By expanding the gabion width, the rotational behavior is suppressed by increasing the frictional resistance of the bottom surface. Furthermore, the bending behavior is also suppressed by the increased bending stiffness of the gabion when its width further expanded.

6. ACKNOWLEDGMENTS

This study was supported by JSPS KAKENHI Grant Number JP17K14723.

7. REFERENCES

[1] Mohri Y., Yasunaka M. and Tani S., Damage to Buried Pipeline Due to Liquefaction-Induced Performance at the Ground by the Hokkaido Nansei-Oki Earthquake in 1993, Proceedings of First International Conference on Earthquake Geotechnical Engineering, IS-Tokyo, 1995, pp. 31–36.

[2] Kawabata T., Sawada Y., Uchida K., Hirai T. and Saito K., Model Tests on Thrust Protecting Method for Buried Bend with Geogrid,

Geosynthetics Engineering Journal, Japan Chapter of International Geosynthetics Society, Vol. 19, 2004, pp. 59–64. (in Japanese)

[3] Kawabata T., Sawada Y., Mohri Y. and Ling I., Dynamic Behavior of Buried Bend with Thrust Restraint in Liquefying Ground, Journal of Japanese Society of Civil Engineering, Vol.67, No. 3, 2011, pp. 399–406. (in Japanese)

[4] Araki H. and Hirakawa D., Model Tests on Thrust Protecting Method for Buried Pipe by Using Geogrid Gabion, Journal of Japanese Society of Civil Engineering, Vol. 74, No. 1, 2018, pp. 106–117. (in Japanese)

[5] Audibert J. M. E. and Nyman K. J., Soil Restraint Against Horizontal Motion of Pipe, Journal of the Geotechnical Engineering Division, Proceedings of the American Society of Civil Engineers, Vol. 103, No. GT10, 1977, pp. 1119–1142.

[6] Itani Y., Fujita N., Sawada Y., Ariyoshi M., Mohri Y. and Kawabata T., Model Experiment on the Horizontal Resistance Force of Buried Pipe in Liquefied Ground, Irrigation, Drainage and Rural Engineering Journal, Vol. 295, 2015, pp. 77–83. (in Japanese)